Received: 2 June 2021 | Revised: 14 September 2021 | Accepted: 17 September 2021

DOI: 10.1111/gcbb.12899

GCB-BIOENERGY BIOPRODUCTS FOR A SUSTAINABLE BIOECONOMY Open Access WILEY

ORIGINAL RESEARCH

# The photosynthetic response of $C_3$ and $C_4$ bioenergy grass species to fluctuating light

**Moon-Sub Lee**[1] | **Ryan A. Boyd**[1] | **Donald R. Ort**[1,2,3]

[1]Carl R. Woese Institute for Genomic Biology, University of Illinois at Urbana-Champaign, Urbana, Illinois, USA

[2]Department of Plant Biology, University of Illinois at Urbana-Champaign, Urbana, Illinois, USA

[3]Department of Crop Science, University of Illinois at Urbana-Champaign, Urbana, Illinois, USA

**Correspondence**
Donald R. Ort, Department of Plant Biology, University of Illinois at Urbana-Champaign, Urbana, IL, USA.
Email: d-ort@illinois.edu

**Funding information**
Biological and Environmental Research, U.S. Department of Energy, Grant/Award Number: DE-SC0018254

**Abstract**

Bioenergy grass species are a renewable energy source, but their productivity has not been fully realized. Improving photosynthetic efficiency has been proposed as a mechanism to increase the productivity of bioenergy grass species. Fluctuating light, experienced by all field grown crops, is known to reduce photosynthetic efficiency. This experiment aimed to evaluate the photosynthetic performance of both $C_3$ and $C_4$ bioenergy grass species under steady state and fluctuating light conditions by examining leaf gas exchange. The fluctuating light regime used here decreased carbon assimilation across all species when compared to expected steady state values. Overall, $C_4$ species assimilated more carbon than $C_3$ species during the fluctuating light regime, with both photosynthetic types assimilating about 16% less carbon than expected based on steady state measurements. Little diversity was observed in response to fluctuating light among $C_3$ species, and photorespiration partially contributed to the rapid decreases in net photosynthetic rates during high to low light transitions. In $C_4$ species, differences among the four NADP-ME species were apparent. Diversity observed among $C_4$ species in this experiment provides evidence that photosynthetic efficiency in response to fluctuating light may be targeted to increase $C_4$ bioenergy grass productivity.

**KEYWORDS**

bioenergy grass, $C_3$ photosynthesis, $C_4$ photosynthesis, fluctuating light, NAD-ME, NADP-ME, PEPCK, photosynthetic efficiency

## 1 | INTRODUCTION

As global human demand for energy increases, bioenergy crops have gained attention as a potential alternative energy source (Langholtz et al., 2016). Bioenergy crops can increase energy security while mitigating environmental problems associated with traditional fossil fuels (Langholtz et al., 2016; Mitchell et al., 2016). To avoid impacting food production on existing agricultural lands, it is important for bioenergy crops to produce consistently high yields (Langholtz et al., 2016; Mitchell et al., 2016). Yield increases may be possible by improving photosynthetic efficiency (Slattery & Ort, 2015). One known source for reduced photosynthetic efficiency is fluctuating light (Chazdon, 1988; Chazdon & Pearcy, 1991; Knapp & Smith, 1989; Kromdijk et al., 2016; Lawson et al., 2012; Pearcy, 1990). In natural environments, plants experience light fluctuation because of shading from overlapping leaves

Moon-Sub Lee and Ryan A. Boyd contributed equally to this work.

within a canopy, wind, passing clouds, and changes in sun angle (Slattery et al., 2018; Vialet-Chabrand et al., 2017). If sufficient variation in photosynthetic efficiency during fluctuating light exists across different bioenergy crops, then these traits can be targeted by future research to improve yields. Because of their high productivity, many grass species are currently being investigated for their utility as bioenergy crops (Jablonowski & Schrey, 2021); however, little is known about how photosynthetic efficiency during fluctuating light varies across these species.

Photosynthesis, the process of using light energy to assimilate $CO_2$, is sensitive to changes in incident light. Changes in light intensity can be rapid, but photosynthetic rates adjust slower, which ultimately affects crop productivity (Slattery et al., 2018). When plants are transitioned from low to high or high to low light intensities, the initial changes in the rate of $CO_2$ assimilation ($A_{net}$) could be related to the processes of electron transport, buildup of metabolite pools, enzyme activities, photoprotection, or stomatal conductance (Kirschbaum & Pearcy, 1988; Sassentath-Cole & Pearcy, 1992, 1994; Way & Pearcy, 2012; Yamori et al., 2012). These limitations likely vary among species and even among cultivars (Acevedo-Siaca et al., 2020; Pignon et al., 2021).

Bioenergy grasses also include both $C_3$ and $C_4$ photosynthetic types, adding another source of variation. Many of the most productive species like *Miscanthus* × *giganteus* and switchgrass use $C_4$ photosynthesis, while other species like giant reed use $C_3$ photosynthesis. $C_4$ species mainly differ from $C_3$ species by operating a $CO_2$ concentrating mechanism (CCM) achieved by the $C_4$ cycle. The CCM increases the $CO_2$ concentration around the enzyme Rubisco. Rubisco serves as the entry point of carbon into $C_3$ cycle by catalyzing the reaction of $CO_2$ with RuBP (Ribulose-1,5-bisphosphate). Both $C_3$ and $C_4$ species use the $C_3$ cycle to produce the chemical energy for cellular respiration as part of the process of photosynthesis. While the addition of the $C_4$ cycle comes with additional costs in the forms of ATP and reducing equivalents (e.g., NADPH) it has benefits. $C_4$ species typically display greater water and nitrogen use efficiency than $C_3$ species (Ghannoum et al., 2010). But how do they compare during fluctuating light?

Slattery et al. (2018) reviewed the impacts of fluctuating light on crop performance and apart from highlighting the previously listed possible limitations, presented contrasting hypotheses for how $C_3$ and $C_4$ species may compare under fluctuating light: $C_4$ species could be more negatively impacted by fluctuating light because increased complexity of the $C_4$ system results in incoordination between metabolic pathways leading to futile cycling of metabolites, or $C_4$ species are less negatively impacted by fluctuating light because the added complexity of the $C_4$ system increases flexibility in the production and consumption of ATP, NADPH, and other redox equivalents (Stitt & Zhu, 2014). Given that Slattery et al. (2018) provided contrasting ideas on the subject, it can be inferred that there is currently no consensus on how the photosynthetic efficiency of $C_3$ and $C_4$ species compare during fluctuating light. Adding yet another source of variation among bioenergy grass species is the $C_4$ subtype (NADP-ME, NAD-ME, and PEPCK), which has also been shown to affect photosynthetic responses to fluctuating light (Laisk & Edwards, 1997).

Here, we examine the changes in photosynthetic leaf gas exchange parameters over time as the leaf transitions between high and low light intensities. The objectives of this study were to (1) quantify photosynthetic efficiency in major bioenergy grasses under both steady state and fluctuating light and (2) contrast $C_3$ and $C_4$ performance under fluctuating light. Six $C_3$ species and six $C_4$ species were included. Of the six $C_4$ species, four were NADP-ME, one was NAD-ME, and one was PEPCK. The experiments presented here will help guide future research on increasing bioenergy grass productivity through altering photosynthetic efficiency.

## 2 | MATERIALS AND METHODS

### 2.1 | Plant materials and growth conditions

Seven bioenergy grass species were selected: *Miscanthus* × *giganteus* (hereafter *M.* × *giganteus*), sugarcane, switchgrass, big bluestem, prairie cordgrass, giant reed, and reed canarygrass. Of these species, only giant reed and reed canarygrass are $C_3$. The $C_3$ species, tall wheatgrass and tall fescue, were also included as they are considered potential bioenergy crops. Wheat, tobacco, and maize were included given that they are commonly measured for leaf gas exchange. Altogether, 12 species were analyzed, including 6 $C_3$ and 6 $C_4$ species. The common name, scientific name, abbreviation, and photosynthetic type of these 12 species are shown in Table 1. *M.* × *giganteus* were collected from the University of Illinois Energy Farm (Lee et al., 2019).

Two separate growth conditions were used in this study, greenhouse and field. For greenhouse experiments, seeds of each species were individually planted at a depth of 3 mm in a propagation tray liner (Nursery Supplies Inc) using Berger BM7 (Berger) as the growing medium, with the exception of *M.* × *giganteus*, which was propagated by rhizomes, and sugarcane and giant reed which were propagated by nodes. After 4 weeks, seedlings were transplanted into pots (30.16 cm diameter × 27.94 cm deep, Nursery Supplies Inc.). All plants were fertilized with granulated fertilizer (Osmocote Plus 13/13/13, The Scotts Company LLC), water-soluble nutrient solution (Peter's Excel 15-5-15,

**TABLE 1** Species examined in this study, photosynthetic pathways, and the experiments species were used in are shown below. The experiments presented are fluctuating light gas exchange in greenhouse grown plants (GH) and field grown plants (Field), the flow rate test of the gas exchange system (FT), and measurements at 2% oxygen ($O_2$)

| Species name | Scientific name | Cultivar/USDA accession | Abbreviation | Type | Subtype | Experiment |
|---|---|---|---|---|---|---|
| Big bluestem | *Andropogon gerardii* Vitman | Bonanza | BB | $C_4$ | NADP-ME | GH. Field, FT |
| Maize | *Zea mays* L. | LG255VT3PRIB | ZM | $C_4$ | NADP-ME | GH, FT |
| *Miscanthus* × *giganteus*[a] | | | MG | $C_4$ | NADP-ME | GH, Field, FT, $O_2$ |
| Sugarcane | *Saccharum spp*. Hybrids | CP88-1762 | SC | $C_4$ | NADP-ME | GH, Field, FT |
| Prairie cordgrass | *Spartina pectinata* L. | Savoy | PC | $C_4$ | PEPCK | GH, Field, FT |
| Switchgrass | *Panicum virgatum* L. | Kanlow | SW | $C_4$ | NAD-ME | GH, Field, FT, $O_2$ |
| Giant reed | *Arundo donax* L. | AL-CA-1 | GR | $C_3$ | — | GH, FT, $O_2$ |
| Reed canarygrass | *Phalaris arundinacea* L. | PI531089 | RC | $C_3$ | — | GH, Field, FT, $O_2$ |
| Tall fescue | *Festuca arundinacea* Schreb | Fawn | TF | $C_3$ | — | GH, Field, FT |
| Tall wheatgrass | *Thinopyrum ponticum* | PI150123 | TW | $C_3$ | — | GH, FT |
| Tobacco | *Nicotiana tabacum* L. | Petit Havana | NT | $C_3$ | — | GH, FT |
| Wheat | *Triticum aestivum* L. | SY007 | TA | $C_3$ | — | GH, FT |

[a]*Miscanthus* × *giganteus* was collected from the University of Illinois Energy Farm (Lee et al., 2019).

Everris NA Inc), and iron chelate supplement (Sprint 330, BASF Corp.) once every 4 weeks. The greenhouse temperature was kept around 27°C (day) and 16°C (night). A 14-h day length was maintained with high-pressure sodium lamps providing an additional 400 μmol $m^{-2}$ $s^{-1}$ photosynthetic photon flux density (PPFD) at canopy level above ambient when necessary. Pots were arranged in a randomized complete block design with four replications. Plants were measured for 2 days at 12 weeks after planting and again for 4 days at 14 weeks after planting.

For the field grown plants, only six species were planted at the University of Illinois Energy Farm: *M.* × *giganteus*, switchgrass, big bluestem, prairie cordgrass, tall fescue, and reed canarygrass (Table 1). The field experimental design was a randomized complete block design with four replications, and blocks were separated by alleys (1.5 m). Four plants of each species were planted in the individual plots (0.9 × 2.7 m). Before field planting in this experiment, plant seeds or rhizomes were transplanted into pots (12.06 cm diameter × 11.74 cm deep, Nursery Supplies Inc.) containing Berger BM7 (Berger) as the growing medium. Plants were grown in a greenhouse for 8 weeks and transplanted by hand in May 2020. Plants were measured for gas exchange 4 weeks after transplanting in field.

## 2.2 | Steady state gas exchange measurements

Light response and $CO_2$ response curves were measured on the youngest fully expanded leaves using a portable infrared gas exchange system (LI-6800, LI-COR Inc.). Leaves were placed in the leaf chamber at 1500 μmol $m^{-2}$ $s^{-1}$ PPFD (LI-6800-01A, LI-COR Inc) at 90% red (635 nm wavelength) and 10% blue (465 nm wavelength). Block temperature was 30°C, flow rate was 500 μmol $s^{-1}$, and relative humidity was 60%. Photosynthetic $CO_2$ response ($A/C_i$) was measured by varying the $CO_2$ reference concentration in the following sequence: 400, 300, 200, 150, 100, 75, 0, 400, 400, 400, 600, 800, 1000, 1200, 1400, and 400 μmol $mol^{-1}$. Light response ($A/Q_{abs}$) was measured on the same leaf following 15–30 min to allow photosynthesis to reach steady state after increasing the light intensity to 2000 μmol $m^{-2}$ $s^{-1}$. For $A/Q_{abs}$ curves, the $CO_2$ sample was maintained at 400 μmol $mol^{-1}$ (~40 Pa) and light intensity was varied as follows: 2000, 1600, 1200, 900, 750, 600, 500, 400, 300, 200, 120, 60, and 20 μmol $m^{-2}$ $s^{-1}$. An additional $A/C_i$ curve was performed at a light intensity of 100 μmol $m^{-2}$ $s^{-1}$ on the same leaf allowing 15–30 min for the leaf to reach steady state. Chamber settings and $CO_2$ concentrations matched the initial $A/C_i$ curve measured at PPFD of 1500 μmol $m^{-2}$ $s^{-1}$. The reference and sample infrared gas analyzers (IRGAs) were matched at every measurement point. For field experiments, measurements were identical except no $A/C_i$ curves were measured at 100 μmol $m^{-2}$ $s^{-1}$ PPFD.

## 2.3 | Fluctuating light gas exchange measurements

Photosynthetic responses to fluctuating light were measured on the same leaf following steady state measurements. The leaf chamber was set to 1500 μmol $m^{-2}$ $s^{-1}$ PPFD. The block

temperature was 30°C, flow rate was 500 μmol $s^{-1}$, the reference $CO_2$ was set to 400 μmol $mol^{-1}$, and $H_2O$ reference was fixed to give an approximate sample RH of 60%. The leaf was allowed 15–30 min at these conditions until photosynthetic rates reached a steady state. A fluctuating light program was written as follows: 1500 μmol $m^{-2}$ $s^{-1}$ PPFD for 4 min, 100 μmol $m^{-2}$ $s^{-1}$ PPFD for 2 min, repeated three additional times, and ending with 1500 μmol $m^{-2}$ $s^{-1}$ for 4 min. Gas exchange data were recorded every 5 s during the 28-min program using default averaging time of 4 s. The IRGAs were matched prior to starting the fluctuating light measurements and were not matched during program to avoid interferences with the 5 s data sampling interval.

## 2.4 | Fluctuating light flow test

The gas exchange system used cannot provide instantaneous measurements of leaf gas exchange. From the manufacturer's application note (https://www.licor.com/env/support/LI-6800/topics/chamber-custom-note.html):

$$C_t = C_e - \left(C_e - C_o\right) e^{-(ft/V)}, \quad (1)$$

where $C_t$ is the chamber concentration at time $t$, $C_e$ is the concentration entering the chamber, $C_o$ is the initial chamber concentration, $f$ is the flow rate, and $V$ is the chamber volume. The chamber volume of LI-6800-01A is 87.3 $cm^3$ (personal communication with manufacturer). We derived the time required to reach 95% ($t_{95}$) of the new concentration as:

$$t_{95} = -\frac{V \ln(0.05)}{f}, \quad (2)$$

such that flow and volume determine the time required to reach the new concentration. As volume of the chamber is constant, four flow rates were tested: 500, 700, 900, and 1100 μmol $s^{-1}$. The calculated time required to reach 95% of the new chamber concentrations was 21, 15, 11, and 9 s, respectively. These calculated equilibration times were longer than our 5 s logging interval and 4 s averaging time. While these calculations were for instantaneous changes in concentrations, we do not expect leaf fluxes of $CO_2$ and $H_2O$ to be instantaneous, but we do want the equilibration time to be faster than the changes in leaf flux. Therefore, we tested the effect of flow rate on fluctuating light measurements. The same starting conditions as listed above were used. After a leaf achieved steady state, it was exposed to 1500 μmol $m^{-2}$ $s^{-1}$ PPFD for 4 min, 100 μmol $m^{-2}$ $s^{-1}$ PPFD for 2 min, then returned to 1500 μmol $m^{-2}$ $s^{-1}$ PPFD for 5 min. The leaf was allowed 15–30 min between each flow rate to return to steady state before starting a new flow rate. Measurements were made 2 weeks after the initial gas exchange measurements at 14 weeks after planting.

## 2.5 | 2% oxygen test

Atmospheric oxygen concentrations are known to affect the net $CO_2$ assimilation rates ($A_{net}$) of leaves. All the above measurements were conducted at 21% $O_2$. To test the effect of oxygen on $A_{net}$ response to fluctuating light, plants were measured at 2% $O_2$. Two $C_3$ species, giant reed and reed canarygrass, and two $C_4$ species, *M.* × *giganteus* and switchgrass, were measured. The above methodology was used for both steady state and fluctuating light measurements except that the air being provided to the leaf came from a 2% $O_2$ gas cylinder balanced in $N_2$ (Airgas USA) connected to the LI-6800 following manufacturer's specifications. Measurements were made 2 weeks after the initial gas exchange measurements at 14 weeks after planting.

## 2.6 | Leaf spectral qualities

Following gas exchange measurements, on the same leaves, leaf absorbance was measured using an integrating sphere (Spectroclip-JAZ-TR, Ocean Optics). Leaf absorbance ($L_A$) was calculated following:

$$L_A = L_I - L_T - L_R, \quad (3)$$

where $L_I$ is the incident radiation, $L_T$ is the transmitted radiation, and $L_R$ is the reflected radiation (400–700 nm). The $L_A$ was used to calculate the amount of incident light that was absorbed for the $A/Q_{abs}$ curves. A SPAD 502 Plus Chlorophyll Meter was also used to characterize the greenness of leaves (Konica Minolta).

## 2.7 | $A/C_i$ curve analysis

$A/C_i$ curves were modeled using the following equation for a non-rectangular hyperbola:

$$A_{net} = \frac{CE\left(C_i - \Gamma\right) + A_{max} - \sqrt{\left(CE\left(C_i - \Gamma\right) + A_{max}\right)^2 - 4\omega CE\left(C_i - \Gamma\right) A_{max}}}{2\omega}, \quad (4)$$

from Bellasio et al. (2016). The observed values of $A_{net}$ and the intercellular $CO_2$ partial pressure ($C_i$) were calculated by the gas exchange system. The carboxylation efficiency (CE) is the initial slope of the $A/C_i$ response. The $CO_2$ compensation point (Γ) is the $C_i$ value where $A_{net}$ is equal to zero. The term $A_{max}$ is the $CO_2$ saturated rate of $A_{net}$. The curvature

factor ($\omega$) is a unitless value ranging between 0 and 1. Model fits were performed in Excel (Microsoft) using the solver add-in to minimize the sum of the differences squared between the observed and modeled values of $A_{net}$ at a given $C_i$, by changing the parameters CE, Γ, $A_{sat}$, and $\omega$. The repeated points at a reference $CO_2$ of 400 μmol $mol^{-1}$ were excluded from model fits, only the first measurement was used. The same model was fit to the $A/C_i$ data collected at 100 μmol $m^{-2}$ $s^{-1}$ PPFD.

## 2.8 | $A/Q_{abs}$ curve analysis

$A/Q_{abs}$ curves were modeled using the following equation for a non-rectangular hyperbola:

$$A_{net} = \frac{\Phi_{CO_2} Q_{abs} + A_{sat} - \sqrt{(\Phi_{CO_2} Q_{abs} + A_{sat})^2 - 4\theta \Phi_{CO_2} Q_{abs} A_{sat}}}{2\theta} - R, \quad (5)$$

from Bellasio et al. (2016) but modified to include respiration ($R$) and absorbed ($Q_{abs}$) rather than incident PPFD ($Q_{in}$). Absorbed PPFD was calculated as:

$$Q_{abs} = Q_{in} \times L_A. \quad (6)$$

The parameters $A_{net}$ and $Q_{in}$ were output by the gas exchange system. The conversion efficiency of converting PPFD into assimilated $CO_2$ ($\Phi_{CO_2}$) is the initial slope of the $A/Q_{abs}$ response. The respiration rate ($R$) is the $y$-intercept of the function when PPFD is equal to zero. The term $A_{sat}$ is the PPFD saturated rate of $A_{net}$. The curvature factor ($\theta$) is a unitless value ranging between 0 and 1. Model fits were performed in Excel (Microsoft) using the solver add-in to minimize the sum of the differences squared between the observed and modeled values of $A_{net}$ at a given PPFD, by changing the parameters $\Phi_{CO_2}$, $R$, $A_{sat}$, and $\theta$.

## 2.9 | Fluctuating light analysis

The observed $A_{net}$ value was reported as $A_{obs}$. The expected $A_{net}$ value, that is, if the leaf could instantaneously reach steady state ($A_{exp}$), was determined using Equations (5 and 6) with $Q_{in}$ for each 5 s data interval. The expected $A_{net}$ value, if stomatal and boundary layer conductance were infinite (i.e., $C_i = C_a$, where $C_a$ is the atmospheric $CO_2$ partial pressure measured by the gas exchange system) and the leaf could reach steady state instantaneously ($A^*_{C_a}$), was calculated using Equation (4) for the appropriate light level (i.e., $A/C_i$ parameters for 1500 or 100 μmol $m^{-2}$ $s^{-1}$) and $C_a$ at each 5 s data interval. The expected $A_{net}$ value, based on observed $C_i$, if the leaf could reach steady state instantaneously ($A^*_{C_i}$), was calculated using Equation (4) for the appropriate light level and $C_i$ at each 5 s data interval. To estimate the carbon lost due to fluctuating photosynthetic rates, $A_{obs}$ was subtracted from $A_{exp}$ at each time point. To estimate the amount of carbon lost due to stomatal limitation and fluctuating photosynthetic rates, $A^*_{C_i}$ was subtracted from $A^*_{C_a}$ similar to Kaiser et al. (2017). To estimate the amount of carbon lost due to non-stomatal limitation and fluctuating photosynthetic rates, $A_{obs}$ was subtracted from $A^*_{C_i}$ similar to Kaiser et al. (2017).

For the high to low light transitions (2 min), low to high light transitions (4 min), and both periods together (6 min), the amount of carbon assimilated ($C_{obs}$, $C_{exp}$, $C^*_{C_a}$, or $C^*_{C_i}$) was calculated as the sum of all $A_{net}$ values ($A_{obs}$, $A_{exp}$, $A^*_{C_a}$, $A^*_{C_i}$, respectively) during the period multiplied by the sampling interval (i.e., 5 s) resulting in units of mmol $m^{-2}$. The four repeated events were treated as technical replicates. For the flow test and 2% $O_2$ test, only the first 40 s were calculated for $C_{obs}$. Values were normalized by dividing the observed value of $A_{net}$ at any given time by the average $A_{net}$ value for the 30 s prior to the first light change ($A_{initial}$).

## 2.10 | Statistical analysis

Experimental design was a randomized complete block design with four replications. Normal distribution and equality of the variances were evaluated using the UNIVARIATE procedure in SAS (SAS institute). If data were not normally distributed, log transformation was performed. Data that met assumptions were analyzed in a mixed-model analysis of variance using PROC MIXED and GLIMMIX procedures in SAS. All statistical significances were determined using Tukey's range test at $\alpha = 0.05$. Datasets of 2% oxygen test were analyzed by a pairwise comparison using SAS at $\alpha = 0.05$ (SAS institute).

# 3 | RESULTS

## 3.1 | Photosynthetic performance during steady state

For greenhouse grown plants, net $CO_2$ assimilation response to intercellular $CO_2$ partial pressure ($A/C_i$) was conducted at high light (1500 μmol $m^{-2}$ $s^{-1}$ PPFD) and low light on all 12 species at 21% $O_2$ (100 μmol $m^{-2}$ $s^{-1}$ PPFD; Figure 1; Figure S1). For modeled $A/C_i$ parameters at high and low light, $C_4$ species had higher CE, lower $CO_2$ compensation point (Γ), and lower $CO_2$ saturated net $CO_2$ assimilation rates ($A_{max}$) compared to $C_3$ species

as expected (Figure 1; Table 2). The fitting of the non-rectangular hyperbola model often resulted in a value of 0 Pa for Γ in $C_4$ species; therefore, the current methodology may not be capable of discerning differences in $C_4$ compensation points among species. Field plants had similar $A/C_i$ responses as greenhouse plants (Figure S1). At 2% $O_2$, $C_4$ species showed no notable changes in their $A/C_i$ response, the $C_3$ species had lower Γ and higher CE compared to measurements at 21% $O_2$ as expected (Figure S1).

For greenhouse grown plants, net $CO_2$ assimilation response to absorbed light ($A/Q_{abs}$) was measured on all 12 species at an atmospheric $CO_2$ partial pressure of 40 Pa and 21% $O_2$ (Figure 1; Figure S2; Table 2). On average, $C_4$ species showed higher light saturated rates of net $CO_2$ assimilation ($A_{sat}$) and respiration rates ($R$) compared to $C_3$ species (Table 2). Leaf spectral characteristics were similar among all species, with only sugarcane and tall fescue having significantly higher light absorbance than tobacco (Table S1). Field measurements of $A/Q_{abs}$ were similar to greenhouse measurements (Figure S2). At 2% $O_2$, $C_3$ species had higher $\Phi_{CO_2}$ and $A_{sat}$ compared to measurements at 21% $O_2$ as expected (Figure S2).

## 3.2 | Photosynthetic performance during fluctuating light

Photosynthetic response to fluctuating light varied among the 12 species of greenhouse grown plants measured at 21% $O_2$ (Figure 2a; Table 3). It was expected based on $A/Q_{abs}$ curves that $C_4$ species would have similar carbon assimilation at low light and higher carbon assimilation at high light compared to $C_3$ species (Figure 2b; Table 3). During high to low light transitions, carbon assimilation was higher than expected due to slow decreases in photosynthetic rates. On average, $A_{net}$ of $C_4$ species decreased slower during high to low light transitions compared to $A_{net}$ of $C_3$ species (Figures 2a and 3; Figure S3). As a result, observed carbon assimilation ($C_{obs}$) during high to low light transitions was higher on average in $C_4$ compared to $C_3$ species (Table 3). $C_4$ species assimilated 118% more carbon than expected, compared to only a 34% increase in $C_3$ species (Table 3, $C_{exp} - C_{obs}$). Neither $C_3$ nor $C_4$ species experienced an overall stomatal ($C^*_{C_a} - C^*_{C_i}$) or non-stomatal limitation ($C^*_{C_i} - C_{obs}$) during the high to low light transition (Figure 2d,e; Table 3).

During low to high light transitions, all species assimilated less carbon than expected (Figure 2; Figure S3; Table 3). On average, $A_{net}$ of $C_4$ species increased similarly during low to high light transitions compared to $A_{net}$ of $C_3$ species (Figures 2a and 3; Figure S3). The observed carbon assimilated during low to high light transitions was greater for $C_4$ compared to $C_3$ species because $C_4$ species had higher $A_{net}$ at high light compared to $C_3$ species as was predicted from $A/Q_{abs}$ curves (Figure 2a,b). Both $C_3$ and $C_4$ species assimilated about 20% less carbon than expected (Table 3). During low to high light transitions $C_4$ species experienced less stomatal limitation ($C^*_{C_a} - C^*_{C_i}$) and similar non-stomatal limitation ($C^*_{C_i} - C_{obs}$) compared to $C_3$ species (Figure 2d,e; Table 3).

Overall, including both high to low and low to high light transitions, both $C_3$ and $C_4$ species assimilated less carbon than expected, losing more carbon from low to high light transitions than was gained from high to low light transitions (Table 3, $C_{exp} - C_{obs}$). $C_3$ species had a highly uniform response to the fluctuating light regime (Figure 3m), while $C_4$ species were highly variable (Figure 3n,o). The NADP-ME subtypes had similar shapes

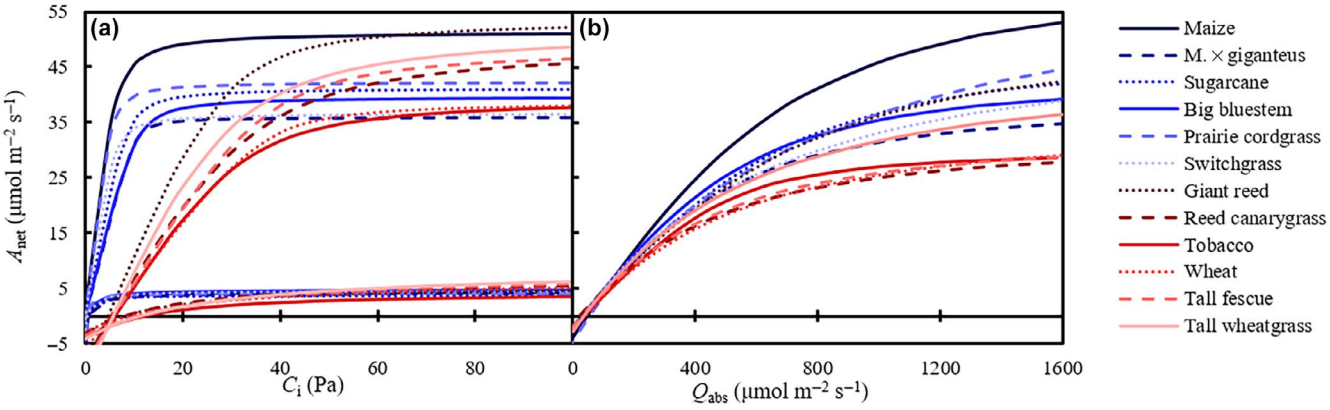


**FIGURE 1** Steady state response of net $CO_2$ assimilation ($A_{net}$). (a) $A_{net}$ response to intercellular $CO_2$ partial pressure ($C_i$) at high (1500 μmol m$^{-2}$ s$^{-1}$) and low (100 μmol m$^{-2}$ s$^{-1}$) light. (b) $A_{net}$ response to absorbed photosynthetic photon flux density ($Q_{abs}$) at atmospheric $CO_2$ concentration of ~40 Pa. Six $C_4$ (blue lines) and six $C_3$ (red lines) species are shown. Lines are the mean of four replicates ($n$) except for wheat where $n = 3$, species as indicated in legend

**TABLE 2** Parameter means for steady state model fits are shown with ±*SE*. For $A/C_i$ curves, $CO_2$ saturated rate of $A_{net}$ ($A_{max}$), the carboxylation efficiency (CE), $CO_2$ compensation point (**Γ**), and the curvature factor ($\omega$) were statistically compared within group ($C_3$ or $C_4$), high and low light were separated. For $A/Q_{abs}$ response, the light saturated rate of $A_{net}$ ($A_{sat}$), the light conversion efficiency for $CO_2$ assimilation ($\Phi_{CO_2}$), respiration rate ($R$), and the curvature factor ($\theta$) were statistically compared within group ($C_3$ or $C_4$). Lower case letters indicate significant differences with group at $\alpha = 0.05$. Group without letters were not significantly different, except for $C_4$ $\theta$, which failed to meet normality assumptions of the statistical test. Species values are the mean of four replicates except for TA, where $n = 3$

| | $A_{max}$ ($\mu$mol m$^{-2}$ s$^{-1}$) | CE ($\mu$mol m$^{-2}$ s$^{-1}$ Pa$^{-1}$) | Γ (Pa) | $\omega$ |
|---|---|---|---|---|
| $A/C_i$ curves at 1500 $\mu$mol m$^{-2}$s$^{-1}$ PPFD | | | | |
| $C_4$ species | | | | |
| BB | 41.56 ± 2.19 ab | 4.90 ± 1.17 ab | 0.00 ± 0.00 | 0.95 ± 0.01 ab |
| MG | 35.75 ± 1.53 b | 3.48 ± 0.17 b | 0.09 ± 0.04 | 0.98 ± 0.01 a |
| PC | 42.06 ± 1.54 ab | 8.42 ± 1.13 a | 0.11 ± 0.07 | 0.90 ± 0.03 b |
| SC | 41.09 ± 3.47 b | 4.59 ± 0.34 b | 0.07 ± 0.07 | 0.95 ± 0.01 ab |
| SW | 35.59 ± 2.65 b | 5.94 ± 0.52 ab | 0.07 ± 0.03 | 0.94 ± 0.02 ab |
| ZM | 51.37 ± 1.10 a | 8.20 ± 0.79 a | 0.07 ± 0.07 | 0.89 ± 0.02 b |
| Mean | 41. 41 ± 1.33 | 5.92 ± 0.48 | 0.07 ± 0.02 | 0.93 ± 0.01 |
| $C_3$ species | | | | |
| GR | 53.29 ± 2.65 | 2.03 ± 0.93 a | 4.73 ± 0.15 c | 0.93 ± 0.03 ab |
| NT | 39.11 ± 0.95 | 1.35 ± 0.90 bc | 6.09 ± 0.26 a | 0.90 ± 0.01 abc |
| RC | 49.01 ± 3.52 | 1.47 ± 0.85 abc | 5.43 ± 0.06 b | 0.85 ± 0.01 bc |
| TA | 38.75 ± 5.22 | 1.17 ± 0.96 c | 5.23 ± 0.09 bc | 0.96 ± 0.01 a |
| TF | 48.52 ± 6.06 | 1.46 ± 0.92 abc | 5.91 ± 0.10 ab | 0.92 ± 0.01 abc |
| TW | 51.83 ± 2.85 | 1.87 ± 0.83 ab | 5.71 ± 0.06 ab | 0.83 ± 0.03 c |
| Mean | 47.10 ± 1.82 | 1.57 ± 0.08 | 5.53 ± 0.11 | 0.90 ± 0.01 |
| $A/C_i$ curves at 100 $\mu$mol m$^{-2}$s$^{-1}$ PPFD | | | | |
| $C_4$ species | | | | |
| BB | 4.69 ± 0.06 | 2.69 ± 0.70 | 0.00 ± 0.00 | 0.00 ± 0.00 |
| MG | 4.16 ± 0.15 | 2.06 ± 0.47 | 0.84 ± 0.09 | 0.00 ± 0.00 |
| PC | 3.99 ± 0.29 | 5.00 ± 1.50 | 0.52 ± 0.12 | 0.00 ± 0.00 |
| SC | 4.47 ± 0.22 | 3.95 ± 1.35 | 0.91 ± 0.53 | 0.24 ± 0.24 |
| SW | 4.47 ± 0.22 | 2.94 ± 0.70 | 0.52 ± 0.21 | 0.00 ± 0.00 |
| ZM | 4.35 ± 0.20 | 3.59 ± 0.18 | 0.71 ± 0.12 | 0.00 ± 0.00 |
| Mean | 4.22 ± 0.12 | 3.37 ± 0.39 | 0.58 ± 0.11 | 0.04 ± 0.04 |
| $C_3$ species | | | | |
| GR | 5.75 ± 0.34 ab | 0.26 ± 0.01 | 8.09 ± 0.07 c | 0.09 ± 0.06 |
| NT | 4.44 ± 0.23 b | 0.19 ± 0.01 | 11.88 ± 0.73 a | 0.09 ± 0.04 |
| RC | 6.64 ± 1.09 ab | 0.28 ± 0.02 | 8.10 ± 0.37 c | 0.12 ± 0.07 |
| TA | 6.70 ± 0.56 ab | 0.23 ± 0.04 | 8.81 ± 0.40 bc | 0.00 ± 0.00 |
| TF | 8.12 ± 0.56 a | 0.24 ± 0.02 | 10.45 ± 0.24 ab | 0.00 ± 0.00 |
| TW | 8.60 ± 1.28 a | 0.25 ± 0.03 | 11.36 ± 0.37 a | 0.03 ± 0.03 |
| Mean | 6.71 ± 0.42 | 0.24 ± 0.01 | 9.83 ± 0.36 | 0.06 ± 0.02 |

(Continues)

but varied in magnitude (Figure 3n). The PEPCK and NAD-ME species showed the most distinctive responses; however, only a single species was measured for each, so it remains to be seen the extent of variability in these subtypes (Figure 3o).

Possible limitations in our methodology could be due to holding $H_2O$ constant. This was done to avoid artifacts that could obscure the true response of the leaf. However, as a result, vapor pressure deficit (VPD) varied during the fluctuating light regime. In this

TABLE 2 (Continued)

| | $A_{sat}$ ($\mu$mol m$^{-2}$ s$^{-1}$) | $\Phi_{CO2}$ mol mol$^{-1}$ | R $\mu$mol m$^{-2}$ s$^{-1}$ | $\theta$ |
|---|---|---|---|---|
| $A/Q_{abs}$ curves at 40 Pa $CO_2$ | | | | |
| $C_4$ species | | | | |
| BB | 48.31 ± 4.85 c | 0.08 ± 0.00 ab | 2.62 ± 0.16 bc | 0.74 ± 0.05 |
| MG | 41.71 ± 1.28 c | 0.07 ± 0.00 b | 2.05 ± 0.16 c | 0.75 ± 0.02 |
| PC | 74.19 ± 1.14 a | 0.09 ± 0.01 a | 4.67 ± 0.31 a | 0.01 ± 0.01 |
| SC | 52.58 ± 3.09 bc | 0.07 ± 0.00 b | 2.98 ± 0.17 bc | 0.75 ± 0.03 |
| SW | 55.25 ± 6.05 bc | 0.08 ± 0.01 ab | 2.92 ± 0.45 bc | 0.31 ± 0.11 |
| ZM | 66.90 ± 3.16 ab | 0.08 ± 0.00 ab | 3.57 ± 0.15 ab | 0.79 ± 0.02 |
| Mean | 56.49 ± 2.65 | 0.08 ± 0.00 | 3.14 ± 0.19 | 0.56 ± 0.06 |
| $C_3$ species | | | | |
| GR | 54.03 ± 0.73 a | 0.06 ± 0.00 | 1.95 ± 0.06 bc | 0.73 ± 0.04 b |
| NT | 32.62 ± 1.40 c | 0.06 ± 0.00 | 2.21 ± 0.17 abc | 0.88 ± 0.01 a |
| RC | 34.36 ± 3.44 bc | 0.06 ± 0.00 | 1.64 ± 0.15 c | 0.60 ± 0.04 bc |
| TA | 39.14 ± 4.86 abc | 0.07 ± 0.01 | 2.75 ± 0.24 a | 0.43 ± 0.03 d |
| TF | 35.33 ± 5.23 bc | 0.06 ± 0.00 | 1.77 ± 0.22 c | 0.63 ± 0.01 bc |
| TW | 47.62 ± 2.66 ab | 0.07 ± 0.01 | 2.58 ± 0.16 ab | 0.51 ± 0.05 cd |
| Mean | 40.58 ± 2.07 | 0.07 ± 0.00 | 2.12 ± 0.10 | 0.64 ± 0.03 |

Abbreviation: PPFD, photosynthetic photon flux density.

experiment, VPD experienced by $C_3$ and $C_4$ species was not drastically different with mean values of 1.60 and 1.74 kPa, respectively. However, VPD may be a confounding factor that needs further experimentation to disentangle from carbon assimilation responses to fluctuating light.

### 3.3 | Flow test for measuring photosynthetic response to fluctuating light

Historically, measurements of $A_{net}$ during non-steady state were conducted using in-house built gas exchange systems with high response times (Laisk & Edwards, 1997; Ruuska et al., 1998). To test the utility of the LI-6800 system for the measurements presented here, four flow rates (500, 700, 900, and 1100 $\mu$mol s$^{-1}$) were tested to determine whether response times of the system were fast enough to capture the rapid changes in leaf gas exchange. Higher flow rates did reveal faster changes in $A_{net}$ during fluctuating light (Figure 3). During high to low light transitions, dips in $A_{net}$ became more pronounced for prairie cordgrass, switchgrass, and all $C_3$ species as flow rate increased (Figure 3e–l). Comparisons among species remained consistent regardless of flow rate (i.e., the general shape of $A_{net}$ response was captured at the lowest flow rate tested; Figure S4).

### 3.4 | Field test for measuring photosynthetic response to fluctuating light

In greenhouses, environmental conditions are controlled. To test that observed $A_{net}$ responses to fluctuating light were not artifacts of greenhouse growth conditions, we also measured our fluctuating light regime on field grown plants. Overall, photosynthetic response from field plants was similar to that of greenhouse grown plants (Figure S3). The delayed or biphasic increase in $A_{net}$ of NADP-ME species observed during low to high light transitions in greenhouse plants was also apparent in field grown big bluestem and *M.* × *giganteus* (Figure S3).

### 3.5 | $O_2$ test for measuring photosynthetic response to fluctuating light

Atmospheric $O_2$ concentrations are known to affect the $A_{net}$ of leaves by altering the rate of Rubisco oxygenation and photorespiratory $CO_2$ release. All the above measurements were conducted at 21% $O_2$. To test the effect of $O_2$ on $A_{net}$ response to fluctuating light two $C_3$ species, giant reed and reed canarygrass, and two $C_4$ species, *M.* × *giganteus* and switchgrass, were

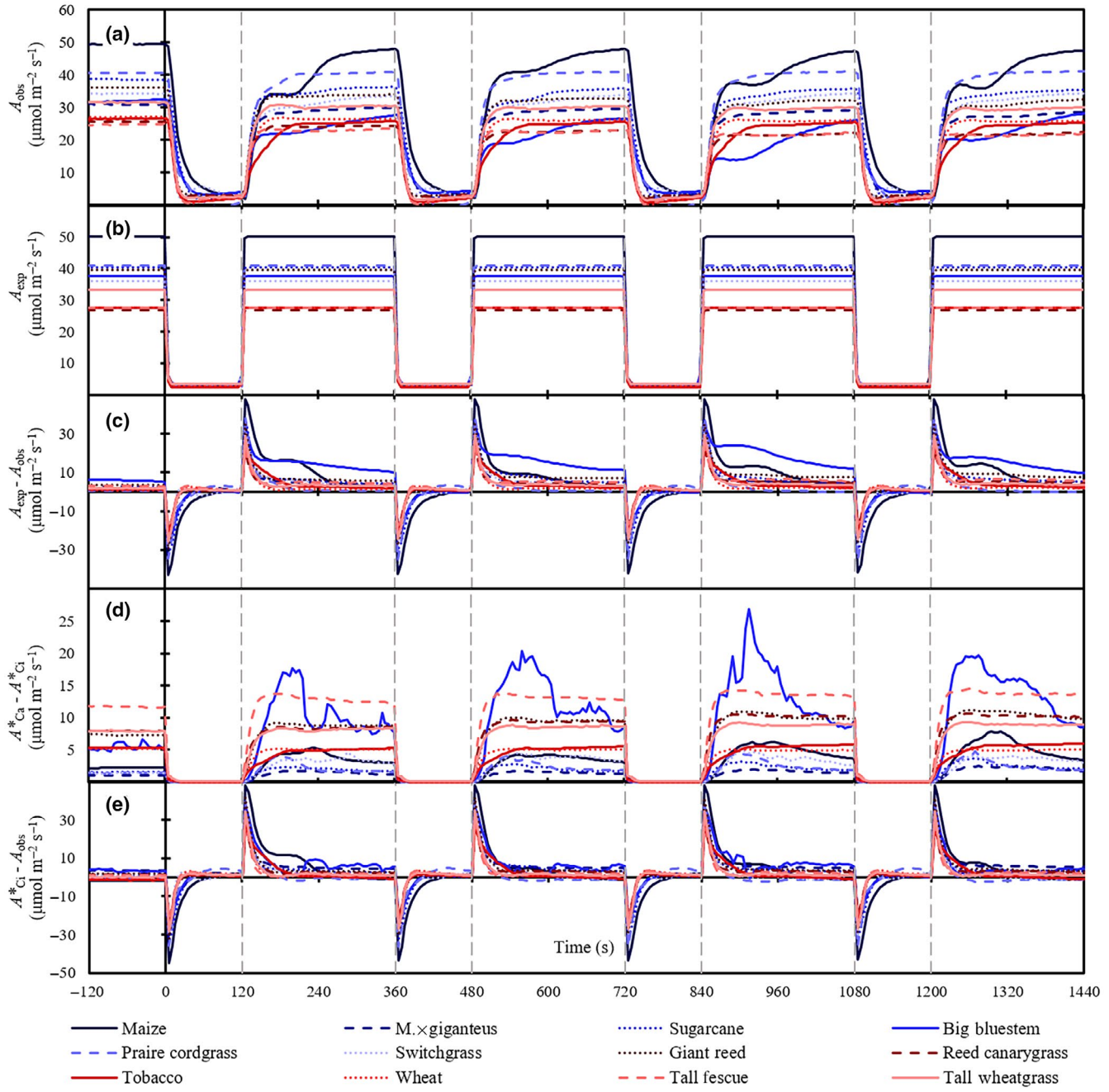


**FIGURE 2** Response of net $CO_2$ assimilation ($A_{net}$) to fluctuating light. (a) The observed response of $A_{net}$ ($A_{obs}$) to 2 min low light (100 μmol m$^{-2}$ s$^{-1}$) and 4 min high light (1500 μmol m$^{-2}$ s$^{-1}$), repeated four times. (b) The expected response of $A_{net}$ to fluctuating light based on $A/Q_{abs}$ curves ($A_{exp}$). (c) The difference between expected and observed $A_{net}$ ($A_{exp} - A_{obs}$). (d) The predicted carbon loss due to stomatal limitation ($A^*_{C_a} - A^*_{C_i}$). (e) The predicted carbon loss due to non-stomatal limitations ($A^*_{C_i} - A_{obs}$). The vertical dotted grey lines indicate each light change. Six $C_3$ species (red lines) and six $C_4$ species (blue lines) are shown. Lines are the mean of four replicates ($n$) except for wheat where $n = 3$

measured at 2% $O_2$. To compare to the rate of change in $A_{net}$ between 21% and 2% $O_2$, an expected value of $A_{net}$ was determined based on 21% $O_2$ data normalized to the mean value of $A_{net}$ at 2% $O_2$ for the 30 s prior the first light transition (Figure 4). $A_{net}$ decreased faster for the two $C_3$ species at 21% $O_2$ compared to 2% $O_2$ with minimal or no change observed in the $C_4$ species. The carbon assimilated during the first 40 s after the high to low light transition was significantly lower at 21% than at 2% $O_2$ in the $C_3$ species (Figure 4e).

**TABLE 3** The carbon assimilated during high to low light, low to high light, or both transitions together (total) are shown for observed ($C_{obs}$) and derived values. $C_{exp}$ is the expected carbon assimilation calculated from $A/Q_{abs}$ curves, $C^*_{C_a}$ is the expected carbon assimilation calculated from $A/C_i$ curves assuming infinite stomatal conductance and steady state, and $C^*_{C_i}$ is the expected carbon assimilation calculated from $A/C_i$ curves using the observed $C_i$ value during fluctuating light. The term $C_{exp} - C_{obs}$ indicates the loss of carbon due to non-steady state, $C^*_{C_a} - C^*_{C_i}$ indicates the loss of carbon due to stomatal limitation and non-steady state, $C^*_{C_i} - C_{obs}$ indicates the loss of carbon due to non-stomatal limitations and non-steady state. Lower case letters indicate significant differences between all species at $\alpha = 0.05$, capital letters indicate differences between the groups ($C_3$, $C_4$). Species values are the mean of four replicates except for TA, where $n = 3$. Standard error is shown

| | $C_{obs}$ | $C_{exp}$ | $C_{exp} - C_{obs}$ | $C^*_{C_a} - C^*_{C_i}$ | $C^*_{C_i} - C_{obs}$ |
|---|---|---|---|---|---|
| | | | mmol $m^{-2}$ | | |
| High to low light transition (2 min) | | | | | |
| $C_4$ species | | | | | |
| BB | 0.86 ± 0.06 b | 0.44 ± 0.02 | −0.42 ± 0.05 cd | 0.01 ± 0.00 abc | −0.34 ± 0.06 cd |
| MG | 0.75 ± 0.03 bc | 0.43 ± 0.03 | −0.32 ± 0.04 bc | 0.01 ± 0.00 bc | −0.29 ± 0.02 bcd |
| PC | 0.64 ± 0.05 bcd | 0.31 ± 0.07 | −0.33 ± 0.03 bc | 0.00 ± 0.00 de | −0.18 ± 0.02 abc |
| SC | 0.86 ± 0.05 b | 0.36 ± 0.04 | −0.50 ± 0.02 d | 0.00 ± 0.00 e | −0.44 ± 0.02 d |
| SW | 0.71 ± 0.05 bc | 0.43 ± 0.02 | −0.27 ± 0.03 bc | 0.01 ± 0.00 cd | −0.20 ± 0.02 abc |
| ZM | 1.29 ± 0.05 a | 0.38 ± 0.02 | −0.91 ± 0.07 e | 0.00 ± 0.00 cde | −0.79 ± 0.06 e |
| $C_3$ species | | | | | |
| GR | 0.65 ± 0.02 bcd | 0.39 ± 0.02 | −0.27 ± 0.01 bc | 0.02 ± 0.00 ab | −0.25 ± 0.02 bcd |
| NT | 0.43 ± 0.02 e | 0.30 ± 0.02 | −0.13 ± 0.01 ab | 0.01 ± 0.00 abc | −0.15 ± 0.02 ab |
| RC | 0.55 ± 0.04 cde | 0.43 ± 0.04 | −0.12 ± 0.02 ab | 0.02 ± 0.00 a | −0.13 ± 0.05 ab |
| TA | 0.42 ± 0.08 e | 0.35 ± 0.05 | −0.07 ± 0.04 a | 0.01 ± 0.00 abc | −0.03 ± 0.04 a |
| TF | 0.46 ± 0.07 de | 0.42 ± 0.03 | −0.03 ± 0.05 a | 0.03 ± 0.00 a | −0.04 ± 0.05 a |
| TW | 0.55 ± 0.04 cde | 0.41 ± 0.05 | −0.15 ± 0.01 a | 0.03 ± 0.01 a | −0.12 ± 0.01 ab |
| $C_4$ | 0.85 ± 0.05 A | 0.39 ± 0.02 | −0.46 ± 0.05 B | 0.00 ± 0.00 B | −0.37 ± 0.05 B |
| $C_3$ | 0.52 ± 0.02 B | 0.38 ± 0.02 | −0.13 ± 0.02 A | 0.02 ± 0.00 A | −0.12 ± 0.02 A |
| Low to high light transition (4 min) | | | | | |
| $C_4$ species | | | | | |
| BB | 5.17 ± 0.81 d | 9.05 ± 0.65 bcd | 3.89 ± 0.21 a | 2.91 ± 0.62 a | 1.72 ± 0.89 |
| MG | 6.48 ± 0.27 cd | 8.02 ± 0.32 b–e | 1.54 ± 0.13 bcd | 0.38 ± 0.19 d | 1.66 ± 0.11 |
| PC | 9.08 ± 0.48 ab | 9.81 ± 0.41 ab | 0.73 ± 0.09 d | 0.58 ± 0.20 bcd | 0.29 ± 0.31 |
| SC | 7.85 ± 0.72 abc | 9.70 ± 0.77 ab | 1.85 ± 0.20 abc | 0.52 ± 0.09 cd | 1.33 ± 0.10 |
| SW | 7.31 ± 0.47 a–d | 8.62 ± 0.59 b–e | 1.31 ± 0.15 bcd | 0.78 ± 0.31 cd | 0.59 ± 0.22 |
| ZM | 9.46 ± 0.20 a | 12.02 ± 0.24 a | 2.57 ± 0.27 ab | 1.08 ± 0.23 bcd | 1.51 ± 0.18 |
| $C_3$ species | | | | | |
| GR | 7.34 ± 0.18 a–d | 9.49 ± 0.24 abc | 2.15 ± 0.16 abc | 2.22 ± 0.29 bcd | 1.37 ± 0.22 |
| NT | 5.40 ± 0.18 d | 6.62 ± 0.21 de | 1.22 ± 0.14 bcd | 1.18 ± 0.13 ab | 0.73 ± 0.05 |
| RC | 5.17 ± 0.37 d | 6.40 ± 0.55 e | 1.23 ± 0.22 cd | 2.21 ± 0.25 ab | 1.00 ± 0.19 |
| TA | 5.93 ± 0.66 cd | 6.64 ± 0.79 cde | 0.71 ± 0.19 d | 1.15 ± 0.24 bcd | 0.60 ± 0.25 |
| TF | 5.12 ± 0.71 d | 6.62 ± 0.91 de | 1.50 ± 0.35 bcd | 3.10 ± 0.24 a | 0.75 ± 0.13 |
| TW | 6.82 ± 0.22 bcd | 8.00 ± 0.31 b–e | 1.18 ± 0.25 cd | 1.98 ± 0.34 abc | 0.72 ± 0.11 |
| $C_4$ | 7.56 ± 0.36 A | 9.54 ± 0.33 A | 1.98 ± 0.22 A | 1.04 ± 0.21 B | 1.18 ± 0.19 |
| $C_3$ | 5.96 ± 0.24 B | 7.32 ± 0.31 B | 1.36 ± 0.12 B | 2.01 ± 0.18 A | 0.87 ± 0.08 |

(Continues)

## 4 | DISCUSSION

Our objective was to quantify natural variation in photosynthetic efficiency of bioenergy grass species. As fluctuating light is a known limitation of photosynthetic efficiency (Slattery et al., 2018), we measured both steady and non-steady state conditions. Steady state measurements separated $C_3$ and $C_4$ species as expected; however,

**TABLE 3** (Continued)

| | $C_{obs}$ | $C_{exp}$ | $C_{exp} - C_{obs}$ | $C^*_{C_a} - C^*_{C_i}$ | $C^*_{C_i} - C_{obs}$ |
|---|---|---|---|---|---|
| | | | mmol $m^{-2}$ | | |
| Total light transition (6 min) | | | | | |
| $C_4$ species | | | | | |
| BB | 6.03 ± 0.87 d | 9.49 ± 0.67 bcd | 3.47 ± 0.25 a | 2.92 ± 0.62 a | 1.38 ± 0.94 |
| MG | 7.23 ± 0.29 bcd | 8.45 ± 0.35 bcd | 1.22 ± 0.13 bc | 0.39 ± 0.19 d | 1.37 ± 0.12 |
| PC | 9.72 ± 0.51 ab | 10.12 ± 0.47 ab | 0.40 ± 0.08 d | 0.58 ± 0.20 cd | 0.11 ± 0.32 |
| SC | 8.71 ± 0.77 abc | 10.06 ± 0.80 ab | 1.35 ± 0.20 bc | 0.52 ± 0.09 cd | 0.90 ± 0.08 |
| SW | 8.02 ± 0.51 bcd | 9.05 ± 0.61 bcd | 1.03 ± 0.12 bc | 0.79 ± 0.31 bcd | 0.39 ± 0.23 |
| ZM | 10.75 ± 0.19 a | 12.40 ± 0.22 a | 1.66 ± 0.21 abc | 1.08 ± 0.23 bcd | 0.72 ± 0.14 |
| $C_3$ species | | | | | |
| GR | 7.99 ± 0.19 bcd | 9.88 ± 0.25 abc | 1.88 ± 0.15 ab | 2.24 ± 0.29 ab | 1.11 ± 0.20 |
| NT | 5.83 ± 0.19 d | 6.92 ± 0.21 d | 1.09 ± 0.14 bc | 1.19 ± 0.13 bcd | 0.58 ± 0.05 |
| RC | 5.73 ± 0.40 d | 6.83 ± 0.59 d | 1.10 ± 0.22 bc | 2.23 ± 0.25 ab | 0.86 ± 0.15 |
| TA | 6.35 ± 0.73 cd | 7.00 ± 0.83 cd | 0.64 ± 0.16 cd | 1.16 ± 0.24 bcd | 0.57 ± 0.22 |
| TF | 5.57 ± 0.78 d | 7.04 ± 0.94 cd | 1.47 ± 0.34 bc | 3.13 ± 0.54 a | 0.71 ± 0.12 |
| TW | 7.37 ± 0.22 bcd | 8.41 ± 0.35 bcd | 1.04 ± 0.27 cd | 2.01 ± 0.34 abc | 0.60 ± 0.12 |
| $C_4$ | 8.41 ± 0.38 A | 9.93 ± 0.33 A | 1.52 ± 0.21 | 1.05 ± 0.22 B | 0.81 ± 0.18 |
| $C_3$ | 6.48 ± 0.26 B | 7.71 ± 0.32 B | 1.23 ± 0.12 | 2.03 ± 0.19 A | 0.75 ± 0.07 |

giant reed outperformed other $C_3$ species having a comparable photosynthetic rate to $C_4$ species at ambient $CO_2$ partial pressures and high light. Under fluctuating light, all species assimilated less carbon than predicted from steady state measurements, supporting the role of fluctuating light in limiting photosynthetic efficiency. $C_3$ species showed little diversity in response of $A_{net}$ to light changes (Figure 3m). The $C_4$ response of $A_{net}$ to fluctuating light varied but known characteristics of photosynthetic subtypes (i.e., NADP-ME, NAD-ME, PEPCK) were observed (Figure 3n,o; Brown & Gracen, 1972; Downton, 1970; Laisk & Edwards, 1997). Among the four NADP-ME species, the response of $A_{net}$ to fluctuating light was diverse (Figure 3n), suggesting that there is potential for trait improvement to increase photosynthetic efficiency of NADP-ME bioenergy grasses.

## 4.1 | Steady state characteristics of $C_3$ and $C_4$ photosynthesis

It is recognized that $C_4$ species have higher photosynthetic efficiency than $C_3$ species under photorespiratory conditions such as higher $O_2$ levels, lower $CO_2$ levels, higher temperatures, and lower water availability because of a CCM (Pearcy & Ehleringer, 1984). Here, we also observed that $C_4$ species in our study displayed higher $A_{sat}$ and CE than $C_3$ species at 21% $O_2$ (Table 2). Of the $C_3$ species we observed, giant reed had the highest CE, highest $A_{sat}$, and lowest Γ (Table 2). At PPFD of 1500 μmol $m^{-2}$ $s^{-1}$, which was used in our fluctuating light regime, giant reed was predicted to have a higher photosynthetic rate than three of the $C_4$ species in this experiment, based on steady state measurements (Figure 1b). Webster et al. (2016) previously reported the higher photosynthetic capabilities of giant reed. Rossa et al. (1998) found that high photosynthetic rates of giant reed may originate from a lack of light saturation of photosynthesis, which we also observed. In our $A/Q_{abs}$ plot, giant reed showed the least amount of light saturation among $C_3$ species, followed by tall wheatgrass, with the remaining four $C_3$ species clustering together (Figure 1b).

## 4.2 | The effect of fluctuating light on carbon assimilation

Fluctuating light is a certainty for field-grown plants, varying in intensity and duration for many reasons including sun angle, wind, shading within canopies, and cloud movement (Knapp & Smith, 1989; Tanaka et al., 2019). During fluctuating light regime employed here, both $C_3$ and $C_4$ species showed excess carbon gain during high to low light transitions, carbon loss during low to high light transitions, for a net loss of carbon when compared to expected values derived from steady state measurements (Table 3). This was observed in greenhouse experiments at 21% $O_2$, 2% $O_2$, and in field

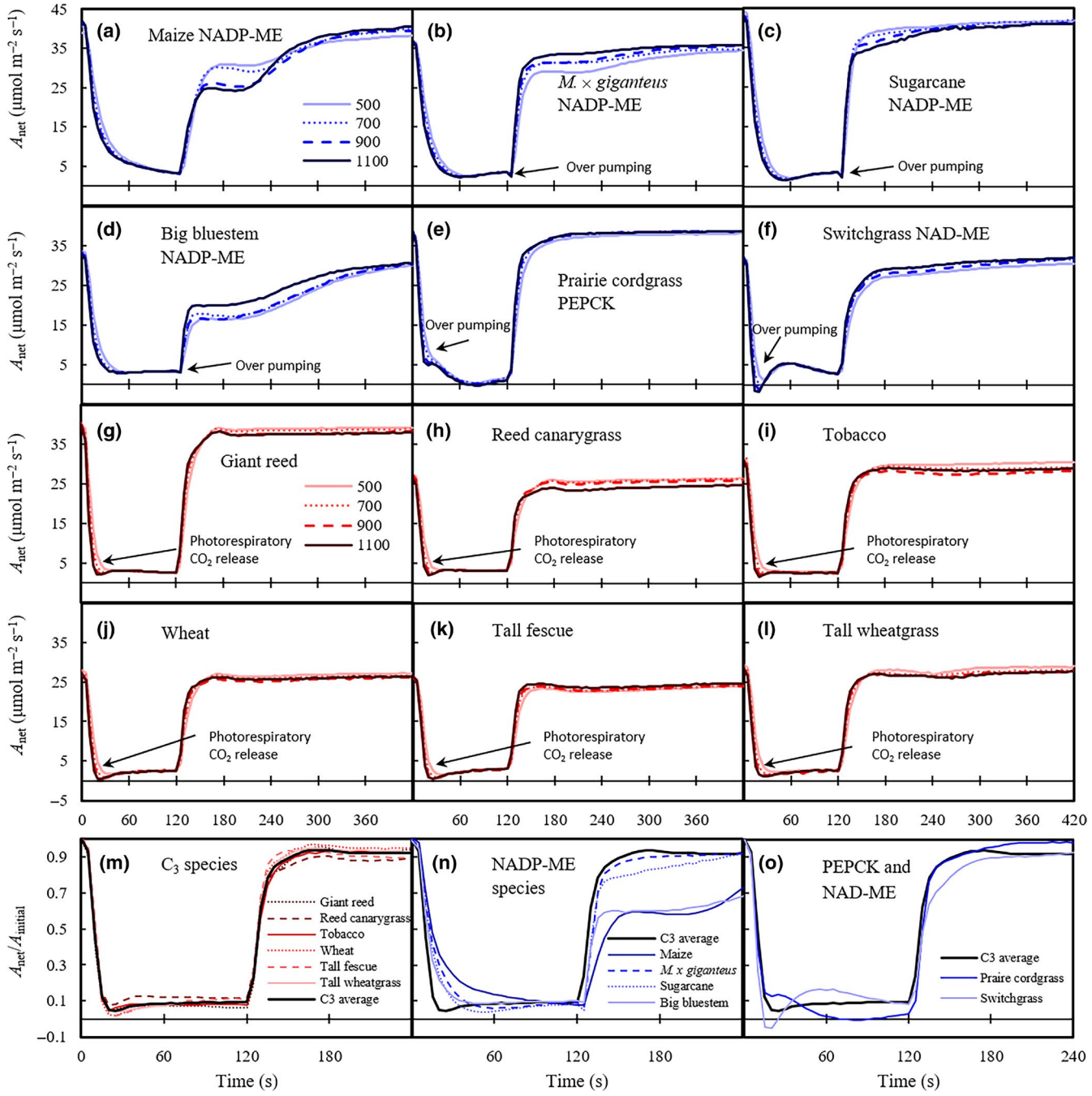


**FIGURE 3** The effect of flow rate on the response of net $CO_2$ assimilation ($A_{net}$) to fluctuating light. (a–l) The change in $A_{net}$ following the transition from a photosynthetic photon flux density of 1500 to 100 μmol $m^{-2}$ $s^{-1}$ at time 0 s and return to high light at 120 s. Line color indicates the flow rate, either 500, 700, 900, or 1100 μmol $s^{-1}$. (m) The $A_{net}/A_{initial}$ for the six $C_3$ species and the average. (n) The $A_{net}/A_{initial}$ for the four NADP-ME subtypes and the $C_3$ average. (o) The $A_{net}/A_{initial}$ for the NAD-ME and PEPCK subtypes and the $C_3$ average. Line color indicates species, and only the highest flow rate (1100 μmol $s^{-1}$) is shown. The $C_4$ species are shown in blue and $C_3$ species are shown in red. Each line is the average of four replicates ($n$) except for wheat where $n = 3$

conditions at 21% $O_2$. The carbon gain during high to low light transitions did not offset the carbon loss during low to high light transitions. The amount of carbon gain during high to low light compared to carbon loss during low to high light likely depends on duration and intensity of light transitions, which was not tested in our study.

## 4.3 | The effect of fluctuating light on $C_3$ and $C_4$ carbon assimilation

The impact of fluctuating light differed between $C_3$ and $C_4$ species. For example, in the initial 40 s during high to low light transitions comparing observed carbon assimilation to the expected value for greenhouse grown plants at

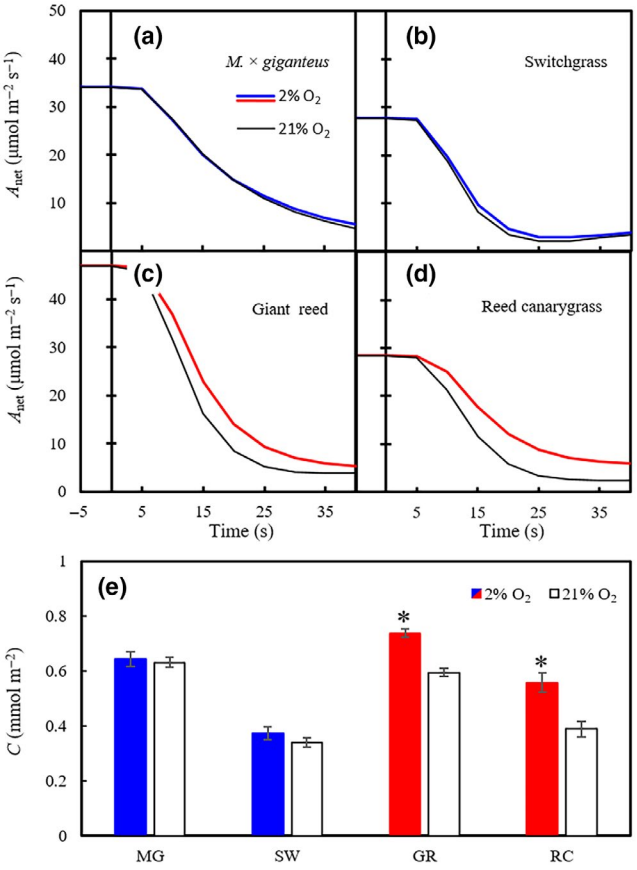


**FIGURE 4** Response of net $CO_2$ assimilation ($A_{net}$) to fluctuating light at 2% $O_2$. (a–d) The first 40 s of a high to low light transition at 2% $O_2$ compared to the expected values at 21% $O_2$. The expected values were calculated by taking the observed values for each species measured at 21% $O_2$ and normalizing them to the $A_{net}$ measured 30 s before the light transition at 2% $O_2$. (e) The carbon assimilated for the first 40 s at both 2% and 21% $O_2$. Asterisk indicates significant differences between 2% and 21% $O_2$. Lines and bars are the mean of the 4 light transition events and 4 biological replicates except for GR, where $n = 3$. Colored lines are 2% $O_2$, black lines are expected values at 21% $O_2$. The $C_4$ species are in blue and the $C_3$ species are in red

21% $O_2$, $C_4$ species assimilated more excess carbon during high to low light (0.46 > 0.21 mmol $m^{-2}$), lost more than expected during low to high light (0.67 > 0.46 mmol $m^{-2}$), but lost less overall than expected (0.20 < 0.25 mmol $m^{-2}$) compared to $C_3$ species (Figure 2, calculations not shown). These calculations, however, were compared to an expected level and did not reflect the actual amount of carbon assimilated. Observation from our highest flow rate (1100 μmol $mol^{-1}$) shows $C_4$ species assimilated more carbon than $C_3$ species during the first 40 s of high to low light transitions (0.62 > 0.33 mmol $m^{-2}$) and low to high light transitions (0.86 > 0.71 mmol $m^{-2}$), giving them an overall higher carbon assimilation (1.48 > 1.04 mmol $m^{-2}$). These comparisons depend on timescale. For example, we observed that $C_3$ species maintained higher $A_{net}$ than $C_4$ species during the first 15 s following a low to high light transition. This short timescale comparison is consistent with findings from Krall and Pearcy (1993), who demonstrated that maize had lower photosynthetic efficiency at light events lasting <10 s when compared to soybean (Pons & Pearcy, 1992).

In general, we found $C_4$ species decrease carbon assimilation rates slower than $C_3$ species during high to low light transitions and increase carbon assimilation rates similarly to $C_3$ species during low to high light transitions. Stitt and Zhu (2014) proposed that large metabolite pools needed to drive diffusion gradients between mesophyll and bundle sheath cells of $C_4$ species can store or release reducing equivalents and ATP with a larger capacity and longer timescale than what is possible in $C_3$ species. Modeling presented by Slattery et al. (2018) suggested that the metabolite buffering capacity of $C_4$ photosynthesis could be capable of sustaining rates of $CO_2$ assimilation for up to 15 s following a high to low light transition. Indeed, there are many examples of $C_4$ species maintaining $A_{net}$ after light changes (Krall & Pearcy, 1993; Laisk & Edwards, 1997; Qiao et al., 2020).

We thought it was likely that the faster reduction of $C_3$ photosynthetic rates during high to low light transitions compared to $C_4$ species could be affected by photorespiration. Because $C_3$ species are subjected to atmospheric concentrations of $CO_2$, high rates of RuBP oxygenation occur compared to $C_4$ species. The resulting products of RuBP oxygenation get partially decarboxylated affecting the net $CO_2$ assimilation rate. The $CO_2$ release from photorespiration is not instantaneous, possibly affecting the $C_3$ responses to fluctuating light. Bulley and Tregunna (1971) found that photorespiratory $CO_2$ release lasts longer than photosynthesis after a sudden decrease in light intensity. Our measurements at 2% $O_2$, which should limit photorespiration, resulted in a slower decline in $A_{net}$ during high to low light transitions and more carbon being assimilated. Suggesting a major limitation to carbon assimilation in $C_3$ species, following a reduction in light intensity, is photorespiratory $CO_2$ release. We have labeled this event in Figure 3g–l. The amount of photorespiration is in part mediated by stomatal conductance which facilitates $CO_2$ movement into the leaf (Lawson et al., 2012). In general, stomatal responses to fluctuating light are slower than observed photosynthetic responses (Lawson et al., 2012; McAusland et al., 2016; Tinoco-Ojanguren & Pearcy, 1993). We observed a higher amount of stomatal limitation ($C^*_{C_a} - C^*_{C_i}$) for $C_3$ species during both light transitions compared to $C_4$ species. This is not surprising as $C_3$ species remain $CO_2$ limited until $C_i$ partial pressures rise above ~60 Pa, whereas $C_4$ species are not limited at $C_i$ values above ~10 Pa, as shown by our $A/C_i$ curves.

Our results of higher $CO_2$ assimilation in $C_4$ species appear contrary to a report of two $C_4$ species performing worse than two $C_3$ species during high to low light transitions

from PPFD of 950 to 95 μmol $m^{-2}$ $s^{-1}$ (Kubásek et al., 2013). Kubásek et al. (2013) suggested that $C_4$ species did worse during fluctuating light compared to $C_3$ species due to mechanisms involving induction of photosynthesis. In their study, plants were started at 50 μmol $m^{-2}$ $s^{-1}$ PPFD, whereas in our fluctuating light regime plants started acclimated to 1500 μmol $m^{-2}$ $s^{-1}$ PPFD. These differences highlight the innumerable ways that light can fluctuate in nature, and that our findings may not be applicable to all fluctuating light comparisons of $C_3$ and $C_4$ species.

### 4.4 | The effect of fluctuating light on carbon assimilation in $C_4$ subtypes

Much previous work on the effect of fluctuating light on $C_4$ species has been done on light to dark transitions (post-illumination), but we observe many similarities to our results presented here. Post-illumination $CO_2$ burst in $C_4$ species are characteristic of NAD-ME and PEPCK type plants (Brown & Gracen, 1972; Downton, 1970). The burst is independent of $O_2$ (Downton, 1970); therefore, it is not a product of photorespiration as is the case for post-illumination $CO_2$ bursts in $C_3$ species (Wynn et al., 1973). The hypothesis is that the $CO_2$ burst results from $CO_2$ leakage from bundle sheath cells, originating from decarboxylation after the $C_3$ cycle has stopped and RuBP has been consumed (Downton, 1970). This process is often called over cycling or over pumping, where more $CO_2$ is released into the bundle sheath than can be used by Rubisco (Furbank et al., 1990; Jenkins et al., 1989; Slattery et al., 2018; von Caemmerer, 2000). We have noted this over pumping event for prairie cordgrass and switchgrass on Figure 3e,f. This explanation also depends on RuBP pool size. If the RuBP pool size is large enough to consume post-illumination $CO_2$ released from the $C_4$ cycle, then it will prevent loss of $CO_2$ from the bundle sheath (Laisk & Edwards, 1997). Because our analysis only included a single NAD-ME and PEPCK species, we do not know how variable this over pumping event might be.

In NADP-ME subtypes, the post-illumination burst is known to be absent (Downton, 1970; Wynn et al., 1973). We also observed gradual decreases in $A_{net}$, lacking observable $CO_2$ bursts, during high to low light transitions for the NADP-ME species observed here: maize, big bluestem, *M.* × *giganteus*, and sugarcane. This is likely because decarboxylation of malate immediately stops in the dark (Laisk & Edwards, 1997). As ATP production stops, phosphoglycerate kinase in the $C_3$ cycle no longer produces substrate needed to produce $NADP^+$ for malate decarboxylation by NADP-ME, which is located in the bundle sheath chloroplasts (Laisk & Edwards, 1997). During high to low light transitions, this suggests tight coupling of $C_4$ and $C_3$ cycles in NADP-ME subtypes, but not NAD-ME or PEPCK subtypes, where the decarboxylase is located outside of bundle sheath chloroplasts (Laisk & Edwards, 1997).

We observed variability among the four NADP-ME species during high to low light transitions. The long persisting $CO_2$ uptake at levels well above expected during high to low light transitions could be due to conversion of 3-PGA to PEP via phosphoglycerate mutase and enolase. In NADP-ME subtypes, PSII activity is reduced in bundle sheath cells, 3-PGA is shuttled to mesophyll cells where it is converted to triose phosphate in reactions that consume ATP and NADPH, triose phosphate is then transported back to the bundle sheath chloroplast providing the ATP and NADPH equivalents to the Calvin cycle (Arrivault et al., 2017; Stitt & Heldt, 1985). If this 3-PGA shuttle can be utilized to produce PEP, then $CO_2$ assimilation can continue without ATP needed to convert pyruvate to PEP (Laisk & Edwards, 1997). The long duration of the higher than expected $A_{net}$ values during high to low light transitions may reflect the time it takes to shuttle metabolites from the bundle sheath chloroplast to PEPC in the mesophyll cytoplasm. This process could explain the different amounts of $C_{obs}$ we observed between NADP-ME species. Maize, which had the highest $C_{obs}$ during high to low light transitions, may have larger 3-PGA pool sizes than *M.* × *giganteus*, sugarcane, and big bluestem. Because differences were observed within subtype, it suggests that traits are available for selection and improvement related to photosynthetic efficiency during high to low light transitions.

During dark to light transitions, previous work has reported a $CO_2$ gulp (rapid increase in $A_{net}$) in NAD-ME and PEPCK subtypes, resulting from the rapid phosphorylation and conversion of alanine to pyruvate to PEP (Laisk & Edwards, 1997). We did not observe an obvious low to high light transition $CO_2$ gulp in either prairie cordgrass or switchgrass, but further measurements with additional species of NAD-ME and PEPCK are needed. During NADP-ME transitions from dark to light, a $CO_2$ burst has been observed (Krall & Pearcy, 1993; Laisk & Edwards, 1997). This is thought to be a result of rapid malate decarboxylation linked to the reduction of large PGA pools. During this initial period, RuBP levels are low and the $CO_2$ released from malate cannot be fixed and leaks out of the bundle sheath (Laisk & Edwards, 1997). This is another example of over pumping. We observed minimal dips in $A_{net}$ for three of the four NADP-ME species measured here within the first 10 s of high light and labeled them in Figure 3b–d.

Given the small size of the $CO_2$ burst, the conditions used during our low to high light transition may have facilitated close coupling of RuBP pools with malate and

3-PGA pools, preventing large losses of $CO_2$ observed in previous studies (Laisk & Edwards, 1997). On the other hand, maize and big bluestem showed a biphasic increase in $A_{net}$ during low to high light transitions, lasting for about 2 min, that was minimal or not consistently observed in *M.* × *giganteus* and sugarcane (Figures 2 and 3). This biphasic increase in $A_{net}$ during low to high light transitions accounts for the biggest limitation to photosynthetic efficiency during fluctuating light in maize and big bluestem. Qiao et al. (2020) suggested this biphasic increase in $A_{net}$ was a result of Rubisco deactivation in maize. However, if that were true, we may expect larger $CO_2$ bursts (i.e., more over pumping) than what we observed in the first 10 s of the low to high light transition. This biphasic response was also observed by Laisk and Edwards (1997), but only at low $CO_2$ concentrations with no hypothesis put forward. We suggest that it could be due to a reestablishment of large metabolite pools needed for forming a concentration gradient between mesophyll and bundle sheath cells. This could also be due to stomatal closure overshoot depressing photosynthesis; however, non-stomatal limitation was higher than stomatal limitation during this time period suggesting biochemical limitations. It should be noted that our estimations for stomatal and non-stomatal limitations are based on steady state and may not reflect what occurs during fluctuating light. Because the biphasic transition from low to high light was not apparent in all four of the NADP-ME species we observed, it could be targeted by future research to improve photosynthetic efficiency of the low to high light transition of NADP-ME bioenergy grass species.

## 5 | CONCLUSION

Understanding natural variation in photosynthetic traits between and among species and cultivars is critical for understanding the regulation of photosynthesis in plants and for providing the necessary knowledge for breeding programs (Flood et al., 2011; Langridge & Fleury, 2011; Tanaka et al., 2019). The diversity we observed in $C_4$ species response to fluctuating light was remarkable compared to the uniformity of the $C_3$ response. The different responses of $C_4$ species during light transitions observed here were related to biochemical subtype of the species and appear to be analogous to previous descriptions of post-illumination measurements in $C_4$ species. Overall, $C_4$ species assimilated more carbon than $C_3$ species for the fluctuating light regime used here, but mismatch between $C_3$ and $C_4$ cycles was evident and variable between species providing targets for future research to increase photosynthetic efficiency during fluctuating light in $C_4$ bioenergy grasses.

## ACKNOWLEDGEMENTS

The information, data, or work presented herein was funded in part by the Biological and Environmental Research (BER) program, U.S. Department of Energy, under Award Number DE-SC0018254. The views and opinions of authors expressed herein do not necessarily state or reflect those of the United States Government or any agency thereof.

## CONFLICT OF INTEREST

The authors declared no conflict of interest.

## DATA AVAILABILITY STATEMENT

The data that support the findings of this study are available from the corresponding author upon reasonable request.

## ORCID

*Moon-Sub Lee* https://orcid.org/0000-0003-3849-5611
*Ryan A. Boyd* https://orcid.org/0000-0003-4009-7700
*Donald R. Ort* https://orcid.org/0000-0002-5435-4387

## REFERENCES

Acevedo-Siaca, L. G., Coe, R., Wang, Y., Kromdijk, J., Quick, W. P., & Long, S. P. (2020). Variation in photosynthetic induction between rice accessions and its potential for improving productivity. *New Phytologist*, *227*(4), 1097–1108. https://doi.org/10.1111/nph.16454

Arrivault, S., Obata, T., Szecówka, M., Mengin, V., Guenther, M., Hoehne, M., Fernie, A. R., & Stitt, M. (2017). Metabolite pools and carbon flow during $C_4$ photosynthesis in maize: $^{13}CO_2$ labeling kinetics and cell type fractionation. *Journal of Experimental Botany*, *68*(2), 283–298. https://doi.org/10.1093/jxb/erw414

Bellasio, C., Beerling, D. J., & Griffiths, H. (2016). An Excel tool for deriving key photosynthetic parameters from combined gas exchange and chlorophyll fluorescence: Theory and practice. *Plant, Cell and Environment*, *39*(6), 1180–1197. https://doi.org/10.1111/pce.12560

Brown, R. H., & Gracen, V. E. (1972). Distribution of the post-illumination $CO_2$ burst among grasses. *Crop Science*, *12*(1), 30–33. https://doi.org/10.2135/cropsci1972.0011183X001200010010x

Bulley, N. R., & Tregunna, E. B. (1971). Photorespiration and the postillumination $CO_2$ burst. *Canadian Journal of Botany*, *49*(8), 1277–1284. https://doi.org/10.1139/b71-181

Chazdon, R. L. (1988). Sunflecks and their importance to forest understory plants. *Advance in Ecological Research*, *18*, 1–63. https://doi.org/10.1016/S0065-2504(08)60179-8

Chazdon, R. L., & Pearcy, R. W. (1991). The importance of sunflecks for forest understory plants. *BioScience*, *41*(11), 760–766. https://doi.org/10.2307/1311725

Downton, W. J. S. (1970). Preferential $C_4$-dicarboxylic acid synthesis, the postillumination $CO_2$ burst, carboxyl transfer step, and grana configurations in plants with $C_4$-photosynthesis. *Canadian Journal of Botany*, *48*(10), 1795–1800. https://doi.org/10.1139/b70-263

Flood, P. J., Harbinson, J., & Aarts, M. G. (2011). Natural genetic variation in plant photosynthesis. *Trends in Plant Science*, *16*(6), 327–335. https://doi.org/10.1016/j.tplants.2011.02.005

Furbank, R. T., Jenkins, C. L. D., & Hatch, M. D. (1990). $C_4$ photosynthesis: Quantum requirement, $C_4$ and overcycling and Q-cycle involvement. *Functional Plant Biology*, *17*(1), 1–7. https://doi.org/10.1071/PP9900001

Ghannoum, O., Evans, J. R., & von Caemmerer, S. (2010). Nitrogen and water use efficiency of $C_4$ plants. In A. Raghavendra & R. Sage (Eds.), *$C_4$ photosynthesis and related $CO_2$ concentrating mechanisms* (pp. 129–146). Springer. https://doi.org/10.1007/978-90-481-9407-0_8

Jablonowski, N. D., & Schrey, S. D. (2021). Bioenergy Crops: Current Status and Future Prospects. *Agronomy*, *11*(2), 316. https://doi.org/10.3390/agronomy11020316

Jenkins, C. L., Furbank, R. T., & Hatch, M. D. (1989). Mechanism of $C_4$ photosynthesis: A model describing the inorganic carbon pool in bundle sheath cells. *Plant Physiology*, *91*(4), 1372–1381. https://doi.org/10.1104/pp.91.4.1372

Kaiser, E., Kromdijk, J., Harbinson, J., Heuvelink, E., & Marcelis, L. F. (2017). Photosynthetic induction and its diffusional, carboxylation and electron transport processes as affected by $CO_2$ partial pressure, temperature, air humidity and blue irradiance. *Annals of Botany*, *119*(1), 191–205. https://doi.org/10.1093/aob/mcw226

Kirschbaum, M. U., & Pearcy, R. W. (1988). Gas exchange analysis of the fast phase of photosynthetic induction in *Alocasia macrorrhiza*. *Plant Physiology*, *87*(4), 818–821. https://doi.org/10.1104/pp.87.4.818

Knapp, A. K., & Smith, W. K. (1989). Influence of growth form on ecophysiological responses to variable sunlight in subalpine plants. *Ecology*, *70*(4), 1069–1082. https://doi.org/10.2307/1941376

Krall, J. P., & Pearcy, R. W. (1993). Concurrent measurements of oxygen and carbon dioxide exchange during lightflecks in maize (*Zea mays* L.). *Plant Physiology*, *103*(3), 823–828. https://doi.org/10.1104/pp.103.3.823

Kromdijk, J., Głowacka, K., Leonelli, L., Gabilly, S. T., Iwai, M., Niyogi, K. K., & Long, S. P. (2016). Improving photosynthesis and crop productivity by accelerating recovery from photoprotection. *Science*, *354*(6314), 857–861. https://doi.org/10.1126/science.aai8878

Kubásek, J., Urban, O., & Šantrůček, J. (2013). $C_4$ plants use fluctuating light less efficiently than do $C_3$ plants: A study of growth, photosynthesis and carbon isotope discrimination. *Physiologia Plantarum*, *149*(4), 528–539. https://doi.org/10.1111/ppl.12057

Laisk, A., & Edwards, G. E. (1997). Post-illumination $CO_2$ exchange and light-induced $CO_2$ bursts during $C_4$ photosynthesis. *Functional Plant Biology*, *24*(4), 517–528. https://doi.org/10.1071/PP97002

Langholtz, M. H., Stokes, B. J., & Eaton, L. M. (2016). *2016 Billion-ton report: Advancing domestic resources for a thriving bioeconomy, Volume 1: Economic availability of feedstock*. Oak Ridge National Laboratory, Oak Ridge, Tennessee, managed by UT-Battelle, LLC for the US Department of Energy, 2016, 1–411.

Langridge, P., & Fleury, D. (2011). Making the most of 'omics' for crop breeding. *Trends in Biotechnology*, *29*(1), 33–40. https://doi.org/10.1016/j.tibtech.2010.09.006

Lawson, T., Kramer, D. M., & Raines, C. A. (2012). Improving yield by exploiting mechanisms underlying natural variation of photosynthesis. *Current Opinion in Biotechnology*, *23*(2), 215–220. https://doi.org/10.1016/j.copbio.2011.12.012

Lee, M. S., Mitchell, R., Heaton, E., Zumpf, C., & Lee, D. K. (2019). Warm-season grass monocultures and mixtures for sustainable bioenergy feedstock production in the Midwest, USA. *BioEnergy Research*, *12*(1), 43–54. https://doi.org/10.1007/s12155-018-9947-7

McAusland, L., Vialet-Chabrand, S., Davey, P., Baker, N. R., Brendel, O., & Lawson, T. (2016). Effects of kinetics of light-induced stomatal responses on photosynthesis and water-use efficiency. *New Phytologist*, *211*(4), 1209–1220. https://doi.org/10.1111/nph.14000

Mitchell, R. B., Schmer, M. R., Anderson, W. F., Jin, V., Balkcom, K. S., Kiniry, J., Coffin, A., & White, P. (2016). Dedicated energy crops and crop residues for bioenergy feedstocks in the central and eastern USA. *Bioenergy Research*, *9*(2), 384–398. https://doi.org/10.1007/s12155-016-9734-2

Pearcy, R. W. (1990). Sunflecks and photosynthesis in plant canopies. *Annual Review of Plant Biology*, *41*(1), 421–453. https://doi.org/10.1146/annurev.pp.41.060190.002225

Pearcy, R. W., & Ehleringer, J. (1984). Comparative ecophysiology of $C_3$ and $C_4$ plants. *Plant, Cell and Environment*, *7*(1), 1–13. https://doi.org/10.1111/j.1365-3040.1984.tb01194.x

Pignon, C. P., Leakey, A. D., Long, S. P., & Kromdijk, J. (2021). Drivers of natural variation in water-use efficiency under fluctuating light are promising targets for improvement in sorghum. *Frontiers in Plant Science*, *12*. https://doi.org/10.3389/fpls.2021.627432

Pons, T. L., & Pearcy, R. W. (1992). Photosynthesis in flashing light in soybean leaves grown in different conditions. II. Lightfleck utilization efficiency. *Plant, Cell and Environment*, *15*(5), 577–584. https://doi.org/10.1111/j.1365-3040.1992.tb01491.x

Qiao, M. Y., Zhang, Y. J., Liu, L. A., Shi, L., Ma, Q. H., Chow, W. S., & Jiang, C. D. (2020). Do rapid photosynthetic responses protect maize leaves against photoinhibition under fluctuating light? *Photosynthesis Research*, *149*, 57–68. https://doi.org/10.1007/s11120-020-00780-5

Rossa, B., Tüffers, A. V., Naidoo, G., & Von Willert, D. J. (1998). *Arundo donax* L. (Poaceae)—A $_C$3 species with unusually high photosynthetic capacity. *Botanica Acta*, *111*(3), 216–221. https://doi.org/10.1111/j.1438-8677.1998.tb00698.x

Ruuska, S., Andrews, T. J., Badger, M. R., Hudson, G. S., Laisk, A., Price, G. D., & von Caemmerer, S. (1998). The interplay between limiting processes in $C_3$ photosynthesis studied by rapid-response gas exchange using transgenic tobacco impaired in photosynthesis. *Functional Plant Biology*, *25*(8), 859–870. https://doi.org/10.1071/PP98079

Sassenrath-Cole, G. F., & Pearcy, R. W. (1992). The role of ribulose-1,5-bisphosphate regeneration in the induction requirement of photosynthetic $CO_2$ exchange under transient light conditions. *Plant Physiology*, *99*(1), 227–234. https://doi.org/10.1104/pp.99.1.227

Sassenrath-Cole, G. F., & Pearcy, R. W. (1994). Regulation of photosynthetic induction state by the magnitude and duration of low light exposure. *Plant Physiology*, *105*(4), 1115–1123. https://doi.org/10.1104/pp.105.4.1115

Slattery, R. A., & Ort, D. R. (2015). Photosynthetic energy conversion efficiency: Setting a baseline for gauging future improvements in important food and biofuel crops. *Plant Physiology*, *168*(2), 383–392. https://doi.org/10.1104/pp.15.00066

Slattery, R. A., Walker, B. J., Weber, A. P. M., & Ort, D. R. (2018). The impacts of fluctuating light on crop performance. *Plant Physiology*, *176*(2), 990–1003. https://doi.org/10.1104/pp.17.01234

Stitt, M., & Heldt, H. W. (1985). Generation and maintenance of concentration gradients between mesophyll cell and bundle sheath in maize leaves. *Biochimica et Biophysica Acta (BBA)-Bioenergetics*, *808*(3), 400–414. https://doi.org/10.1016/0005-2728(85)90148-3

Stitt, M., & Zhu, X. G. (2014). The large pools of metabolites involved in intercellular metabolite shuttles in $C_4$ photosynthesis provide enormous flexibility and robustness in a fluctuating light environment. *Plant, Cell and Environment*, *37*(9), 1985–1988. https://doi.org/10.1111/pce.12290

Tanaka, Y., Adachi, S., & Yamori, W. (2019). Natural genetic variation of the photosynthetic induction response to fluctuating light environment. *Current Opinion in Plant Biology*, *49*, 52–59. https://doi.org/10.1016/j.pbi.2019.04.010

Tinoco-Ojanguren, C., & Pearcy, R. W. (1993). Stomatal dynamics and its importance to carbon gain in two rainforest Piper species: II. Stomatal versus biochemical limitations during photosynthetic induction. *Oecologia*, *94*(3), 395–402. https://doi.org/10.1007/BF00317115

Vialet-Chabrand, S., Matthews, J. S., Simkin, A. J., Raines, C. A., & Lawson, T. (2017). Importance of fluctuations in light on plant photosynthetic acclimation. *Plant Physiology*, *173*(4), 2163–2179. https://doi.org/10.1104/pp.16.01767

von Caemmerer, S. (2000). *Biochemical models of leaf photosynthesis*. CSIRO Publishing.

Way, D. A., & Pearcy, R. W. (2012). Sunflecks in trees and forests: From photosynthetic physiology to global change biology. *Tree Physiology*, *32*(9), 1066–1081. https://doi.org/10.1093/treephys/tps064

Webster, R. J., Driever, S. M., Kromdijk, J., McGrath, J., Leakey, A. D., Siebke, K., Demetriades-Shah, T., Bonnage, S., Peloe, T., Lawson, T., & Long, S. P. (2016). High $C_3$ photosynthetic capacity and high intrinsic water use efficiency underlies the high productivity of the bioenergy grass *Arundo donax*. *Scientific Reports*, *6*(1), 1–10. https://doi.org/10.1038/srep20694

Wynn, T., Brown, H., Campbell, W. H., & Black, C. C. (1973). Dark release of $^{14}CO_2$ from higher plant leaves. *Plant Physiology*, *52*(3), 288–291. https://doi.org/10.1104/pp.52.3.288

Yamori, W., Masumoto, C., Fukayama, H., & Makino, A. (2012). Rubisco activase is a key regulator of non-steady-state photosynthesis at any leaf temperature and to a lesser extent, of steady-state photosynthesis at high temperature. *The Plant Journal*, *71*(6), 871–880. https://doi.org/10.1111/j.1365-313X.2012.05041.x

## SUPPORTING INFORMATION

Additional supporting information may be found in the online version of the article at the publisher's website.

**How to cite this article:** Lee, M.-S., Boyd, R. A., & Ort, D. R. (2021). The photosynthetic response of $C_3$ and $C_4$ bioenergy grass species to fluctuating light. *GCB Bioenergy*, 00, 1–17. https://doi.org/10.1111/gcbb.12899